Search for $\nu_\mu \to \nu_e$ oscillations with the OPERA experiment in the CNGS beam

The OPERA collaboration

E-mail: akitaka.ariga@lhep.unibe.ch

ABSTRACT: A first result of the search for $\nu_\mu \to \nu_e$ oscillations in the OPERA experiment, located at the Gran Sasso Underground Laboratory, is presented. The experiment looked for the appearance of ν_e in the CNGS neutrino beam using the data collected in 2008 and 2009. Data are compatible with the non-oscillation hypothesis in the three-flavour mixing model. A further analysis of the same data constrains the non-standard oscillation parameters θ_{new} and Δm^2_{new} suggested by the LSND and MiniBooNE experiments. For large Δm^2_{new} values ($>0.1\,\text{eV}^2$), the OPERA 90% C.L. upper limit on $\sin^2(2\theta_{\text{new}})$ based on a Bayesian statistical method reaches the value 7.2×10^{-3}.

This paper is dedicated to the memory of Prof. Perihan Tolun.

Contents

1 Introduction

The OPERA experiment [1] is designed to perform an appearance search for the $\nu_\mu \to \nu_\tau$ oscillations [2, 3] in the CNGS ν_μ beam [4] produced at CERN and directed towards the OPERA detector at the Gran Sasso Underground Laboratory (LNGS), 730 km away. A charged-current (CC) ν_τ interaction in the lead-emulsion target can be identified by detecting the decay of the short-lived τ lepton through particle tracking in the high-resolution nuclear emulsions. The observation of two ν_τ candidate events has recently been reported [5–7]. The tracking capabilities of emulsions also allow to identify electrons produced in CC interactions of ν_e and therefore to search for ν_e appearance from $\nu_\mu \to \nu_e$ oscillations. Given the long baseline of the experiment, and the high energy of the ν_μ beam ($\langle E \rangle = 17\,\text{GeV}$), OPERA has a good sensitivity for $\Delta m^2 > 0.01\,\text{eV}^2$, i.e. for the LSND [8]–MiniBooNE [9] allowed region (see section 4.3). Recently ICARUS, which shares the beamline with OPERA, severely limited this region [10]. Here we present a further constraint on these non-standard oscillations from the analysis of the data collected in 2008 and 2009.

2 Detector, beam and data taking

In OPERA, neutrinos interact in a large mass target made of lead plates interspaced with nuclear emulsion films acting as high accuracy tracking devices [11–13]. This kind of target is historically called Emulsion Cloud Chamber (ECC). The full OPERA detector is made of a veto plane followed by two identical Super Modules (SM), each consisting of a target section and a magnetic muon spectrometer. The target sections are made of, in total,
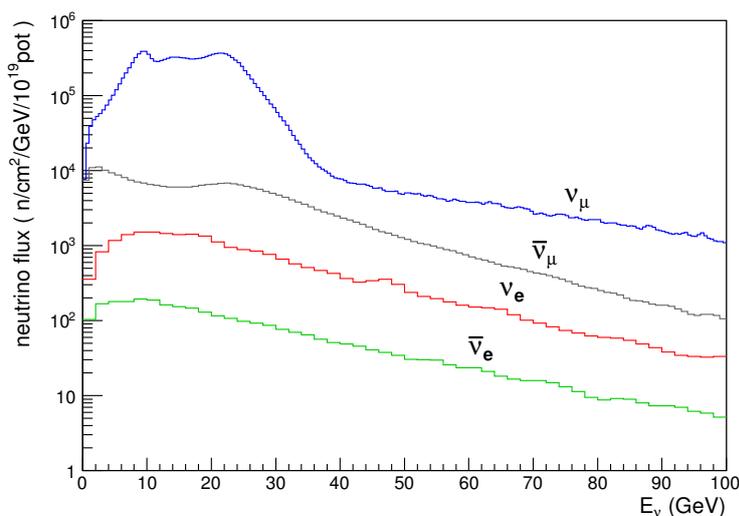
Figure 1. Neutrino fluxes of the different components at Gran Sasso in log scale.

150,000 emulsion/lead ECC modules (or "bricks") arranged in planes, with a weight of about 1,250 tons, interleaved by the scintillator "Target Tracker" (TT) planes. A target brick consists of 56 1-mm thick lead plates interleaved with 57 emulsion films for a total weight of 8.3 kg. Its thickness along the beam direction corresponds to about 10 X_0, which is optimized to detect $\nu_\mu \rightarrow \nu_\tau$ oscillations. Tightly packed removable doublets of emulsion films, called Changeable Sheets (CS) [14], are placed on the downstream face of each brick. They serve as interfaces between the TT planes and the bricks to facilitate the location of the neutrino interactions.

Charged particles from a neutrino interaction in a brick cross the CS and produce signals in the scintillator strips of the TT. These signals are used to trigger the read-out and identify the brick where the interaction occurred. The brick is then extracted by an automated system. After development, the emulsion films are sent to the scanning laboratories.

The CNGS ν_μ beam, to which the OPERA detector is exposed, contains a small contamination of $\overline{\nu}_\mu$, ν_e , and $\overline{\nu}_e$. The energy spectra at the detector, as obtained from a Monte Carlo simulation [15], are shown in figure 1. The integrated contamination of ν_e and $\overline{\nu}_e$ CC interactions at Gran Sasso, relative to the integrated number of ν_μ CC interactions, is 0.88% and 0.05%, respectively.

OPERA collected data corresponding to 17.97×10^{19} protons on target (pot) by December 2012 with 18941 events recorded. The analysis reported in this paper uses the data collected in 2008 and 2009, corresponding to 5.25×10^{19} pot (1.73×10^{19} and 3.52×10^{19} pot, respectively) and to 5255 events recorded. The details of data taking and a comparison with Monte Carlo (MC) simulations for the 2008 and 2009 runs are reported in [6, 16].
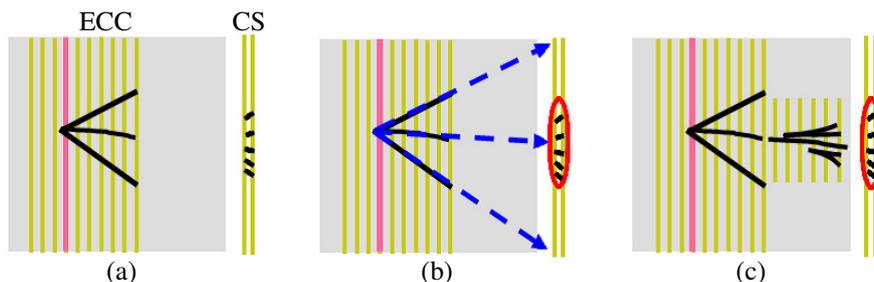
Figure 2. Sketch for the procedure of a systematic search for ν_e candidates. After the reconstruction of tracks in the standard volume (a), all tracks emerging from the interaction vertex (the pink film) are extrapolated to the CS (b). If 3 or more tracks are found in the CS, corresponding to a given track, an additional volume along the full track length is scanned, leading to the detection of the electromagnetic shower (c).

3   Emulsion scanning and search for ν_e interactions

Bricks that are candidates for containing neutrino interactions are analysed following a complex procedure described in detail in [5, 6]. Here we just recall the main steps of the analysis.

The TT predictions are used for a large area scan of the corresponding CS films. If candidate tracks corresponding to the TT predictions are found in the CS, the 57 films contained in the brick are developed, and sent to the scanning labs. The tracks found in the CS are then followed upstream from film to film (scan-back) to find the neutrino interaction vertex. Once the vertex is found, the scanning of a volume downstream of the vertex (1 cm^2 in area and at least 7 films or 1.2 X$_0$ in thickness) is performed in order to reconstruct all the tracks connected to the vertex and to search for decay topologies.

The main goal is the observation of the decay of a τ lepton, as a signature for a ν_τ CC interaction. Moreover, the scanning also allows identifying electrons, hence ν_e CC interactions. The identification of an electron is essentially based on the detection of the associated electromagnetic shower. Since the size of the standard scanned volume is too short in the beam direction to contain the electromagnetic shower, the search for electrons is performed using an extended scanning volume defined by a dedicated procedure sketched in figure 2. All primary tracks emerging from the interaction vertex are extrapolated to the CS. The tracks with angles similar ($\Delta\theta < 150$ mrad) to that of the corresponding primary track (figure 2b) are searched in the CS region within 2 mm around the projected point. If 3 or more tracks are found in the CS, corresponding to a given primary track, an additional volume along the candidate track is scanned, aiming at the reconstruction of an electromagnetic shower (figure 2c).

If a shower is found, the corresponding primary track becomes an electron candidate. The candidate track is then carefully inspected in the first two emulsion films following the interaction vertex. The aim is to check whether the track is due to a single particle (an electron) or to an e^+e^- pair and so to reject electromagnetic showers initiated by the early conversion of a γ from a π^0 decay. Figure 3 shows, as an example, the reconstruction of an
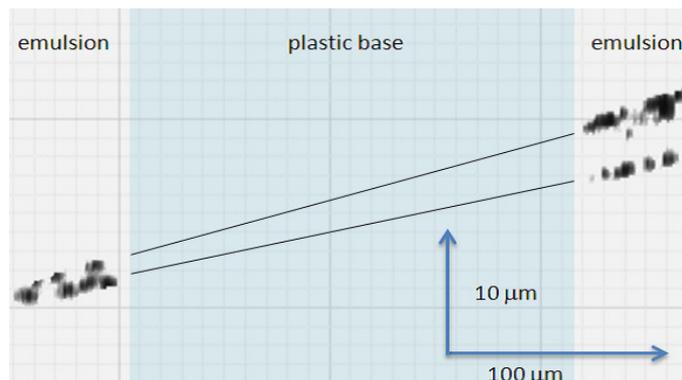
Figure 3. Side view of an e^+e^- pair detected in an emulsion film. Note, that in a film the two emulsion layers are separated by a 205 μm thick plastic base.

e^+e^- pair from a γ conversion in the two layers of one emulsion film. The figure illustrates the capability to measure tracks with micrometric resolution. To remove γ background, those configurations are excluded where a track can be separated into two almost parallel segments more than 1 μm apart in the first or second film.

A significant impact parameter of the electron track with respect to the primary vertex would allow to identify the event as a ν_τ CC interaction with a $\tau \to e$ decay. For the present analysis, an upper limit of 10 μm is set on this impact parameter to select tracks originating from the vertex.

In addition, a scan-back procedure along the electromagnetic shower, described in [1], is applied. Implemented to increase the detection efficiency for a $\tau \to e$ decay in the ν_τ quasi-elastic interactions, it is also beneficial for the detection of ν_e CC interactions.

Once the presence of an electron track is confirmed at the neutrino interaction vertex, the event is classified as a ν_e interaction. The energy of the ν_e candidates is estimated from the reconstructed energy deposition in the TT making use of a calibration obtained through the MC simulation in a similar way as for the ν_μ CC and neutral-current (NC) events as described in [16]. The estimated energy resolution for an energy range up to 100 GeV can be parametrized as:

$$\Delta E/E = 0.37 + 0.74/\sqrt{E} \ \ (E \text{ in GeV}).$$

Among the 5255 candidate neutrino interactions collected during the 2008 and 2009 runs, 2853 vertices were localized in the bricks, out of which 505 did not have a muon identified by the electronic detectors, i.e. were not classified as ν_μ CC interactions. Out of those 505 events 19 ν_e candidate events were found; 17 events were found with the procedure illustrated in figure 2, and the 2 remaining events were found with the scan-back procedure mentioned before. To illustrate the typical pattern of ν_e candidates, figure 4 shows the reconstructed image of a ν_e candidate event, with the track segments observed along the showering electron track.

The ν_e detection efficiency as a function of the neutrino energy is computed with a GEANT3 based MC simulation. The simulated events are reconstructed with the same
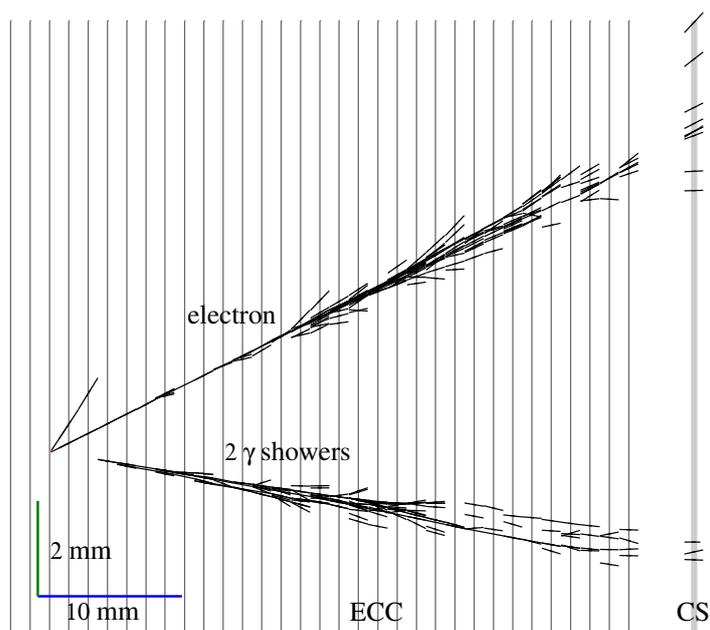
Figure 4. Display of the reconstructed emulsion tracks of one of the ν_e candidate events. The reconstructed neutrino energy is 32.5 GeV. Two tracks are observed at the neutrino interaction vertex. One of the two generates an electromagnetic shower and is identified as an electron. In addition, two showers from γ conversions are observed (overlapping in this projection), starting from 2 and 3 films downstream of the vertex.

algorithms as used for the data. The results of the simulation are shown in figure 5. The efficiency drop at low energy is strongly related to the smaller number of hits in the TT and the CS, due to the absorption of electromagnetic showers in the bricks. In order to optimize the performance of the experiment, the scanning and analysis strategies were tuned along the years. All strategies are tested in the MC and the deviations are taken as systematic uncertainties. Larger deviations are observed at lower energy, depending on the number of tracks observed in the CS. For events with energy above 10 GeV, the systematic uncertainty is estimated to be 10% and 20% below. Averaged over its energy spectrum, the ν_e beam contamination detection efficiency is $\varepsilon_{\text{det}} = (53 \pm 5)\%$. For neutrino energies smaller than 30 GeV (20 GeV) it is $\varepsilon_{\text{det}} = (43 \pm 5)\%$ $((35 \pm 4)\%)$.

Apart from the ν_e background associated to the beam contamination (see section 4), two main sources of background are considered for the ν_e search: (a) π^0 misidentified as electron in neutrino interactions without a reconstructed muon; (b) ν_τ CC interactions with the decay of the τ into an electron.

Background (a) occurs if an e^+e^- pair appears to be connected to the interaction vertex and cannot be distinguished from a single particle in the first two emulsion films after the vertex or if one branch of the pair has a very low energy and remains undetected. This background was evaluated directly from the data. In 1106 neutrino interactions, γs converting in the second and third lead plates after the interaction vertex were searched for, and the above described procedure was applied to them; 1 event passed the criteria
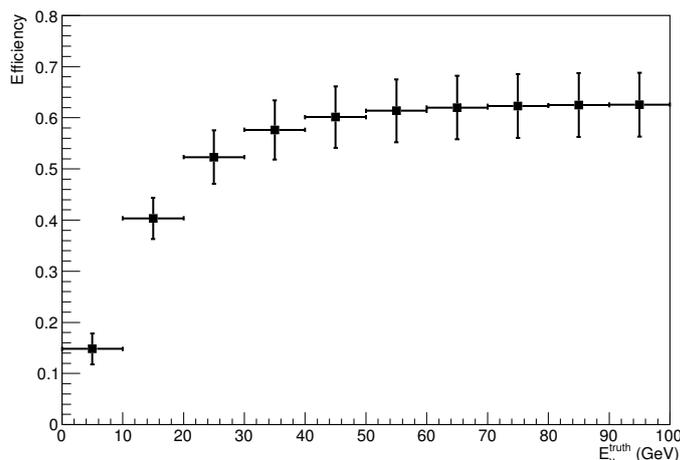
Figure 5. Detection efficiency of ν_e events as a function of the neutrino energy, obtained from MC simulations. The error bars show the estimated systematic uncertainties.

for the ν_e search. This result was converted into the probability to observe background ν_e candidates due to γ conversions in the first lead plate, taking into account the radiation length. By normalizing to our sample, the estimated background (a) is 0.2 ± 0.2 events. This number is compatible with an independent MC evaluation. The effect of π^0 decays to a Dalitz pair is estimated to be one order of magnitude smaller than the above value; therefore it is neglected.

Background (b) was computed by MC simulation assuming the three-flavour $\nu_\mu \to \nu_\tau$ oscillation at maximal mixing and $\Delta m^2 = 2.32 \times 10^{-3} \, \text{eV}^2$ [17]. This background comes mainly from τ decaying in the same lead plate as the primary vertex with the impact parameter of the daughter electron to the primary vertex smaller than 10 μm; secondarily from an undetected kink ($\theta_{kink} < 20$ mrad) from τ decaying in further downstream material. Background (b) is estimated to be 0.3 ± 0.1 events in our sample.

The total amount of the considered background for the ν_e CC interaction search is 0.4 ± 0.2 events.

4 Oscillation analysis

4.1 Background to $\nu_\mu \to \nu_e$ appearance

A signal for $\nu_\mu \to \nu_e$ oscillations should appear as a significant excess of electron events with respect to the expected background, mainly due to ν_e and $\overline{\nu}_e$ CC interactions from the beam contamination. A detailed evaluation of this number was performed, starting from the fluxes of the different beam components presented in figure 1. The simulation of the neutrino fluxes and spectra including a description of all beam line elements is based on the FLUKA MC code [18, 19]. Details on the simulation can be found in [20]. Conservatively a 10% systematic uncertainty on the ν_e beam contamination has been considered as in [10]. However it is worth noting that this number affects marginally the sensitivity of the mea-

Energy cut		20 GeV	30 GeV	No cut
BG common to both analyses	BG (a) from π^0	0.2	0.2	0.2
	BG (b) from $\tau \to e$	0.2	0.3	0.3
	ν_e beam contamination	4.2	7.7	19.4
Total expected BG in 3-flavour oscillation analysis		4.6	8.2	19.8
BG to non-standard oscillation analysis only	ν_e via 3-flavour oscillation	1.0	1.3	1.4
Total expected BG in non-standard oscillation analysis		5.6	9.4	21.3
Data		4	6	19

Table 1. Expected and observed number of events for the different energy cuts.

surement which is dominated by the small sample size. The fluxes were weighted with the CC cross sections and the energy dependent detection efficiency. An additional inefficiency of 6% (for 2008) and 3% (for 2009) was introduced to reflect the lower film quality of a small fraction of the bricks. Taking into account the target mass and the pot corresponding to our data, we expect to observe 19.4 ± 2.8 (syst) ν_e events from the beam contamination in the full energy range. Together with the backgrounds (a) and (b) discussed above, we expect 19.8 ± 2.8 (syst) background ν_e events. This number is in agreement with the 19 observed candidate ν_e events and therefore the room for oscillations is reduced. In the following we analyse two scenarios.

4.2 Three-flavour mixing scenario

A non-zero θ_{13} has recently been reported by several experiments [21–24]. Using the following oscillation parameters [17]: $\sin^2(2\theta_{13}) = 0.098$, $\sin^2(2\theta_{23}) = 1$, $\Delta m_{32}^2 = \Delta m_{31}^2 = 2.32 \times 10^{-3}\,\mathrm{eV}^2$, also assuming $\delta_{CP} = 0$ and neglecting matter effects, 1.4 oscillated ν_e CC events are expected to be detected in the whole energy range.

Figure 6 shows the reconstructed energy distribution of the 19 ν_e candidates, compared with the expected reconstructed energy spectra from the ν_e beam contamination, the oscillated ν_e from the three-flavour oscillation and the background (a) and (b), normalized to the pot analysed for this paper. To increase the signal to background ratio a cut $E < 20\,\mathrm{GeV}$ is applied on the reconstructed energy of the event, which provides the best figure of merit on the sensitivity to θ_{13}. Within this cut, 4.2 events from ν_e beam contamination and 0.4 events from the backgrounds (a) and (b) are expected, while 4 events are observed. The numbers are summarized in table 1. The number of observed events is compatible with the non-oscillation hypothesis and an upper limit $\sin^2(2\theta_{13}) < 0.44$ is derived at the 90% Confidence Level (C.L.).

4.3 Non-standard oscillations

Beyond the three-neutrino paradigm, some possible hints for non-standard effects have been reported, in particular by the LSND [8] and MiniBooNE [9] experiments. We have used OPERA data to set an upper limit on non-standard $\nu_\mu \to \nu_e$ oscillations.

We used the conventional approach of expressing the $\nu_\mu \to \nu_e$ oscillation probability in the one mass scale dominance approximation, given by the following formula with new

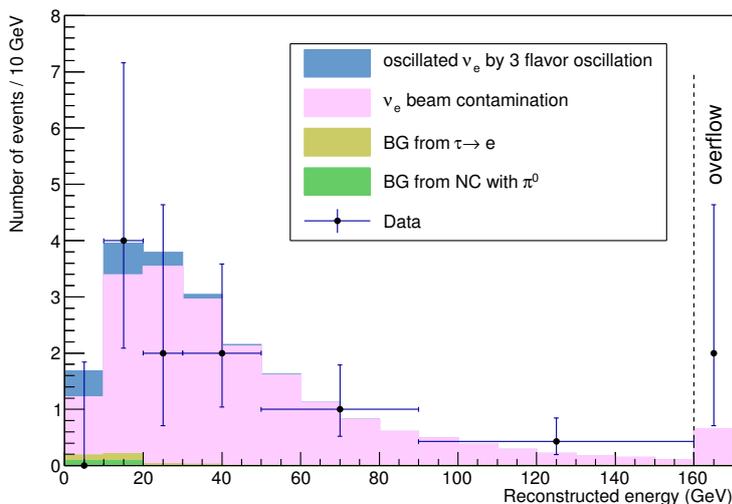**Figure 6**. Distribution of the reconstructed energy of the ν_e events, and the expected spectrum from the different sources in a stack histogram, normalized to the number of pot analysed for this paper.

oscillation parameters θ_{new} and Δm_{new}^2:

$$P_{\nu_\mu \to \nu_e} = \sin^2(2\theta_{\text{new}}) \cdot \sin^2(1.27\Delta m_{\text{new}}^2 L(\text{km})/E(\text{GeV}))$$

Note however that this approach does not allow a direct comparison between experiments working in different L/E regimes [25].

The ν_μ flux at the detector, normalized to the integrated statistics used in our analysis, is weighted by the oscillation probability, by the CC cross-section and by the energy dependent detection efficiency, to obtain the number of ν_e CC events expected from this oscillation.

As the energy spectrum of the oscillated ν_e with large Δm_{new}^2 ($>0.1\,\text{eV}^2$) follows the spectrum of ν_μ, which is basically vanishing above $40\,\text{GeV}$ (see figure 1), a cut on the reconstructed energy is introduced. The optimal cut on the reconstructed energy in terms of sensitivity is found to be $30\,\text{GeV}$. We observe 6 events below $30\,\text{GeV}$ (69% of the oscillation signal at large Δm_{new}^2 is estimated to remain in this region), while the expected number of events from background is estimated to be 9.4 ± 1.3 (syst) (see table 1). Note that we choose to include the three-flavour oscillation induced events into the background. In this case, the oscillation probability does not contain the θ_{13} driven term.

The 90% C.L. upper limit on $\sin^2(2\theta_{\text{new}})$ is then computed by comparing the expectation from oscillation plus backgrounds, with the observed number of events. Since we observed a smaller number of events than the expected background, we provide both, the Feldman and Cousins (F&C) confidence intervals [26] and the Bayesian bounds, setting a prior to zero in the unphysical region and to a constant in the physical region [27]. Uncertainties of the background were incorporated using prescriptions provided in [17]. The results obtained from the two methods for the different C.L. are reported in table 2. We

		Upper limit		Sensitivity	
	C.L.	F&C	Bayes	F&C	Bayes
Number of oscillated	90%	3.1	4.5	6.1	6.5
ν_e events	95%	4.3	5.7	7.8	7.9
	99%	6.7	8.2	10.7	10.9
$\sin^2(2\theta_{\text{new}})$ at	90%	5.0×10^{-3}	7.2×10^{-3}	9.7×10^{-3}	10.4×10^{-3}
large Δm^2	95%	6.9×10^{-3}	9.1×10^{-3}	12.4×10^{-3}	12.7×10^{-3}
	99%	10.6×10^{-3}	13.1×10^{-3}	17.1×10^{-3}	17.4×10^{-3}

Table 2. Upper limits on the number of oscillated ν_e CC events and $\sin^2(2\theta_{\text{new}})$, obtained by the F&C and Bayesian methods, for C.L. 90%, 95%, 99%. The sensitivity is computed assuming that the number of observed events is 9, which is the closest integer to the 9.4 expected background events.

	Upper limit		Sensitivity	
Energy cut	F&C	Bayes	F&C	Bayes
20 GeV	8.5×10^{-3}	10.4×10^{-3}	14.2×10^{-3}	14.2×10^{-3}
30 GeV	5.0×10^{-3}	7.2×10^{-3}	9.7×10^{-3}	10.4×10^{-3}
No cut	8.6×10^{-3}	9.5×10^{-3}	10.8×10^{-3}	11.0×10^{-3}

Table 3. 90% C.L. upper limits and sensitivities on $\sin^2(2\theta_{\text{new}})$, for different energy cuts, according to the F&C and Bayesian methods.

also quote our sensitivity calculated assuming 9 observed events (integer number closest to the expected background).

Given the underfluctuation of the data, the curve with the Bayesian upper limit was chosen for the exclusion plot shown in figure 7. For convenience, results from the other experiments, working at different L/E regimes, are also reported in this figure. For large Δm^2_{new} values the OPERA 90% upper limit on $\sin^2(2\theta_{\text{new}})$ reaches the value 7.2×10^{-3}, while the sensitivity corresponding to the pot used for this analysis is 10.4×10^{-3}.

As seen in figure 6, the underfluctuation is mainly present in the low energy region. In order to illustrate the impact of energy cuts on our analysis, in table 3, the limits are quoted for different cuts.

5 Conclusions and perspectives

First results of a search for $\nu_\mu \to \nu_e$ oscillations with the OPERA experiment at the Gran Sasso Underground Laboratory have been presented. The experiment searched for the appearance of ν_e in the CNGS neutrino beam using the data collected in 2008 and 2009, corresponding to an integrated intensity of 5.25×10^{19} pot. The observation of 19 ν_e candidate events is compatible with the non-oscillation expectation of 19.8 ± 2.8 events.

The current result on the search for the three-flavour neutrino oscillation yields an upper limit $\sin^2(2\theta_{13}) < 0.44$ (90% C.L.).
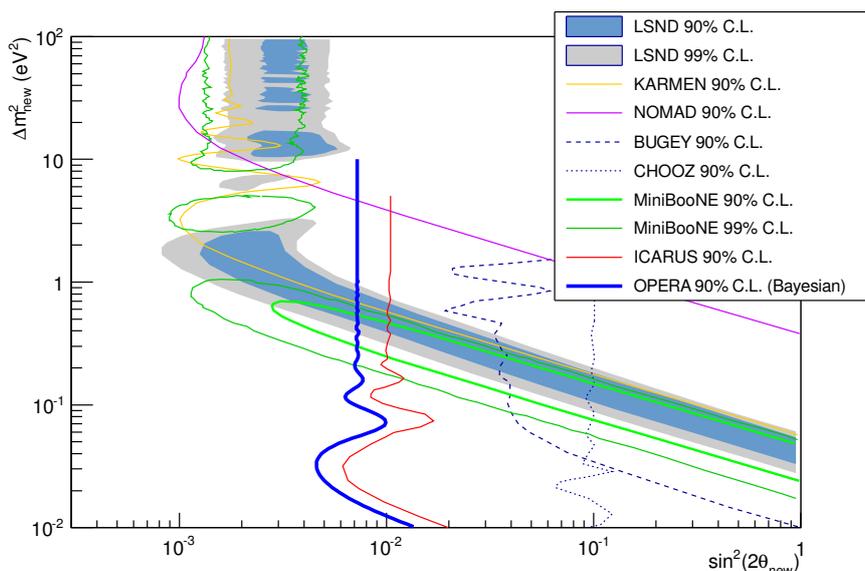
Figure 7. The exclusion plot for the parameters of the non-standard $\nu_\mu \rightarrow \nu_e$ oscillation, obtained from this analysis using the Bayesian method, is shown. The other limits shown, mostly using frequentist methods, are from KARMEN ($\overline{\nu}_\mu \rightarrow \overline{\nu}_e$ [28]), BUGEY ($\overline{\nu}_e$ disappearance [29]), CHOOZ ($\overline{\nu}_e$ disappearance [30]), NOMAD ($\nu_\mu \rightarrow \nu_e$ [31]) and ICARUS ($\nu_\mu \rightarrow \nu_e$ [10]). The regions corresponding to the positive indications reported by LSND ($\overline{\nu}_\mu \rightarrow \overline{\nu}_e$ [8]) and MiniBooNE ($\nu_\mu \rightarrow \nu_e$ and $\overline{\nu}_\mu \rightarrow \overline{\nu}_e$ [9]) are also shown.

OPERA limits the parameter space available for a non-standard ν_e appearance suggested by the results of the LSND and MiniBooNE experiments. It further constrains the still allowed region around $\Delta m^2_{\text{new}} = 5 \times 10^{-2} \text{ eV}^2$. For large Δm^2_{new} values, the 90% C.L. upper limit on $\sin^2(2\theta_{\text{new}})$ reaches 7.2×10^{-3}. This result is still affected by the statistical underfluctuation, the sensitivity corresponding to the analysed statistics being 10.4×10^{-3}. A Bayesian statistical treatment has therefore been adopted for determining the upper limit.

Various improvements are expected for the future. The statistics will be increased by a factor of 3.4 by completing the analysis of the collected data. The reconstructed energy resolution will be improved when the calorimetric measurement in the TT will be complemented by following the hadron tracks and the electron showers in the downstream bricks.

With the increase in sample size and the improvements in the analysis, the effect of a possible statistical underfluctuation of the background will be reduced and OPERA should then be able to access the parameter region comparable to its sensitivity below $\sin^2(2\theta_{\text{new}}) = 5.0 \times 10^{-3}$.

Acknowledgments

References

[1] OPERA collaboration, M. Guler et al., *An appearance experiment to search for $\nu_\mu \to \nu_\tau$ oscillations in the CNGS beam: experimental proposal*, CERN-SPSC-2000-028, CERN, Geneva Switzerland (2000) [LNGS-P25-00].

[2] B. Pontecorvo, *Mesonium and anti-mesonium*, *Sov. Phys. JETP* **6** (1957) 429 [INSPIRE].

[3] Z. Maki, M. Nakagawa and S. Sakata, *Remarks on the unified model of elementary particles*, *Prog. Theor. Phys.* **28** (1962) 870 [INSPIRE].

[4] *CNGS webpage*, http://proj-cngs.web.cern.ch/proj-cngs.

[5] OPERA collaboration, N. Agafonova et al., *Observation of a first ν_τ candidate in the OPERA experiment in the CNGS beam*, *Phys. Lett.* **B 691** (2010) 138 [arXiv:1006.1623] [INSPIRE].

[6] OPERA collaboration, *Search for $\nu_\mu \to \nu_\tau$ oscillation with the OPERA experiment in the CNGS beam*, *New J. Phys.* **14** (2012) 033017 [arXiv:1107.2594] [INSPIRE].

[7] OPERA collaboration, M. Nakamura et al., *Results from OPERA*, talk given at the *Neutrino 2012 Conf.*, Kyoto, Japan (2012).

[8] LSND collaboration, A. Aguilar-Arevalo et al., *Evidence for neutrino oscillations from the observation of $\bar{\nu}_e$ appearance in a $\bar{\nu}_\mu$ beam*, *Phys. Rev.* **D 64** (2001) 112007 [hep-ex/0104049] [INSPIRE].

[9] MINIBOONE collaboration, A. Aguilar-Arevalo et al., *A Combined $\nu_\mu \to \nu_e$ and $\bar{\nu}_\mu \to \bar{\nu}_e$ Oscillation Analysis of the MiniBooNE Excesses*, arXiv:1207.4809 [INSPIRE].

[10] M. Antonello, B. Baibussinov, P. Benetti, E. Calligarich, N. Canci et al., *Experimental search for the "LSND anomaly" with the ICARUS detector in the CNGS neutrino beam*, *Eur. Phys. J.* **C 73** (2013) 2345 [arXiv:1209.0122] [INSPIRE].

[11] R. Acquafredda, T. Adam, N. Agafonova, P. Alvarez Sanchez, M. Ambrosio et al., *The OPERA experiment in the CERN to Gran Sasso neutrino beam*, 2009 *JINST* **4** P04018 [INSPIRE].

[12] N. Agafonova, A. Anokhina, S. Aoki, A. Ariga, T. Ariga et al., *The Detection of neutrino interactions in the emulsion/lead target of the OPERA experiment*, 2009 *JINST* **4** P06020 [arXiv:0903.2973] [INSPIRE].

[13] T. Nakamura, A. Ariga, T. Ban, T. Fukuda, T. Fukuda et al., *The OPERA film: New nuclear emulsion for large-scale, high-precision experiments*, *Nucl. Instrum. Meth.* **A 556** (2006) 80 [INSPIRE].

[14] OPERA collaboration, A. Anokhina et al., *Emulsion sheet doublets as interface trackers for the OPERA experiment*, 2008 *JINST* **3** P07005 [arXiv:0804.1985] [INSPIRE].

[15] *CNGS neutrino flux calculations webpage*, http://www.mi.infn.it/~psala/Icarus/cngs.html.

[16] OPERA collaboration, N. Agafonova et al., *Study of neutrino interactions with the electronic detectors of the OPERA experiment*, *New J. Phys.* **13** (2011) 053051 [arXiv:1102.1882] [INSPIRE].

[17] PARTICLE DATA GROUP collaboration, J. Beringer et al., *Review of Particle Physics (RPP)*, *Phys. Rev.* **D 86** (2012) 010001 [INSPIRE].

[18] A. Ferrari, P.R. Sala, A. Fassò, J. Ranft, *FLUKA: a multi-particle transport code (program version 2005)*, *CERN-2005-010* (2005) [INFN/TC 05/11].

[19] A. Fasso, A. Ferrari, S. Roesler, P. Sala, F. Ballarini et al., *The Physics models of FLUKA: Status and recent developments*, *eConf* **C 0303241** (2003) MOMT005 [hep-ph/0306267] [INSPIRE].

[20] A. Ferrari, A.M. Guglielmi, M. Lorenzo-Sentis, S. Roesler, P.R. Sala, L. Sarchiapone, *An updated Monte Carlo calculation of the CNGS neutrino beam*, CERN-AB-Note-2006-038 (2007).

[21] DAYA-BAY collaboration, F. An et al., *Observation of electron-antineutrino disappearance at Daya Bay*, *Phys. Rev. Lett.* **108** (2012) 171803 [arXiv:1203.1669] [INSPIRE].

[22] RENO collaboration, J. Ahn et al., *Observation of Reactor Electron Antineutrino Disappearance in the RENO Experiment*, *Phys. Rev. Lett.* **108** (2012) 191802 [arXiv:1204.0626] [INSPIRE].

[23] DOUBLE-CHOOZ collaboration, Y. Abe et al., *Indication for the disappearance of reactor electron antineutrinos in the Double Chooz experiment*, *Phys. Rev. Lett.* **108** (2012) 131801 [arXiv:1112.6353] [INSPIRE].

[24] T2K collaboration, K. Abe et al., *Indication of Electron Neutrino Appearance from an Accelerator-produced Off-axis Muon Neutrino Beam*, *Phys. Rev. Lett.* **107** (2011) 041801 [`arXiv:1106.2822`] [ɪɴSPIRE].

[25] B. Bhattacharya, A.M. Thalapillil and C.E. Wagner, *Implications of sterile neutrinos for medium/long-baseline neutrino experiments and the determination of* θ_{13}, *Phys. Rev.* **D 85** (2012) 073004 [`arXiv:1111.4225`] [ɪɴSPIRE].

[26] G.J. Feldman and R.D. Cousins, *A Unified approach to the classical statistical analysis of small signals*, *Phys. Rev.* **D 57** (1998) 3873 [`physics/9711021`] [ɪɴSPIRE].

[27] G. Cowan, *Statistical Data Analysis*, Clarendon Press, Oxford (1998).

[28] KARMEN collaboration, B. Armbruster et al., *Upper limits for neutrino oscillations* $\bar{\nu}_\mu \to \bar{\nu}_e$ *from muon decay at rest*, *Phys. Rev.* **D 65** (2002) 112001 [`hep-ex/0203021`] [ɪɴSPIRE].

[29] Y. Declais, J. Favier, A. Metref, H. Pessard, B. Achkar et al., *Search for neutrino oscillations at 15-meters, 40-meters and 95-meters from a nuclear power reactor at Bugey*, *Nucl. Phys.* **B 434** (1995) 503 [ɪɴSPIRE].

[30] CHOOZ collaboration, M. Apollonio et al., *Limits on neutrino oscillations from the CHOOZ experiment*, *Phys. Lett.* **B 466** (1999) 415 [`hep-ex/9907037`] [ɪɴSPIRE].

[31] NOMAD collaboration, P. Astier et al., *Search for* $\nu_\mu \to \nu_e$ *oscillations in the NOMAD experiment*, *Phys. Lett.* **B 570** (2003) 19 [`hep-ex/0306037`] [ɪɴSPIRE].

The OPERA collaboration

N. Agafonova,[a] A. Aleksandrov,[b] A. Anokhina,[c] S. Aoki,[d] A. Ariga,[e,*] T. Ariga,[e]
D. Autiero,[f] A. Badertscher,[g] A. Ben Dhahbi,[e] A. Bertolin,[h] C. Bozza,[i] R. Brugnera,[h,j]
F. Brunet,[k] G. Brunetti,[e] B. Buettner,[l] S. Buontempo,[b] L. Chaussard,[f] M. Chernyavsky,[m]
V. Chiarella,[n] A. Chukanov,[o] L. Consiglio,[b,q] N. D'Ambrosio,[p] G. De Lellis,[b,q] M. De Serio,[r,s]
P. del Amo Sanchez,[k] A. Di Crescenzo,[b,q] D. Di Ferdinando,[t] N. Di Marco,[p] S. Dmitrievsky,[o]
M. Dracos,[u] D. Duchesneau,[k] S. Dusini,[h] T. Dzhatdoev,[c] J. Ebert,[l] A. Ereditato,[e]
T. Ferber,[l,1] R.A. Fini,[r] T. Fukuda,[v] A. Garfagnini,[h,j] G. Giacomelli,[w,t] C. Goellnitz,[l]
J. Goldberg,[x] Y. Gornushkin,[o] G. Grella,[i] F. Grianti,[y,n] A.M. Guler,[z] C. Gustavino,[aa]
C. Hagner,[l] K. Hamada,[ab] T. Hara,[d] M. Hierholzer,[l,2] A. Hollnagel,[l] B. Hosseini,[b,q]
H. Ishida,[v] K. Ishiguro,[ab] K. Jakovcic,[ac] C. Jollet,[u] F. Juget,[e,3] C. Kamiscioglu,[z,ad]
M. Kamiscioglu,[z] J. Kawada,[e] J.H. Kim,[ae] S.H. Kim,[ae,4] M. Kimura,[e] N. Kitagawa,[ab]
B. Klicek,[ac] K. Kodama,[af] M. Komatsu,[ab] U. Kose,[h] I. Kreslo,[e] A. Lauria,[b,q] J. Lenkeit,[l]
A. Ljubicic,[ac] A. Longhin,[n] P. Loverre,[aa,ag] A. Malgin,[a] C. Mancini-Terracciano,[e,5]
G. Mandrioli,[t] J. Marteau,[f] T. Matsuo,[v] V. Matveev,[a] N. Mauri,[n] E. Medinaceli,[h,j]
F.W. Meisel,[e] A. Meregaglia,[u] P. Migliozzi,[b] S. Mikado,[v] A. Minotti,[ag,6] P. Monacelli,[ah]
M.C. Montesi,[b,q] K. Morishima,[ab] M.T. Muciaccia,[r,s] M. Nakamura,[ab] T. Nakano,[ab]
Y. Nakatsuka,[ab] D. Naumov,[o] K. Niwa,[ab] S. Ogawa,[v] N. Okateva,[m] A. Olchevsky,[o]
T. Omura,[ab] K. Ozaki,[d] A. Paoloni,[n] B.D. Park,[ae,7] I.G. Park,[ae] A. Pastore,[r] L. Patrizii,[t]
E. Pennacchio,[f] H. Pessard,[k] C. Pistillo,[e] D. Podgrudkov,[c] N. Polukhina,[m] M. Pozzato,[w,t]
K. Pretzl,[e] F. Pupilli,[p] R. Rescigno,[i] M. Roda,[h,j] T. Roganova,[c] H. Rokujo,[d] G. Rosa,[aa,ag]
I. Rostovtseva,[ai] A. Rubbia,[g] A. Russo,[b] O. Ryazhskaya,[a] O. Sato,[ab] Y. Sato,[aj]
T. Schchedrina,[b] A. Schembri,[p] W. Schmidt-Parzefall,[l] I. Shakiryanova,[a] A. Sheshukov,[b]
H. Shibuya,[v] T. Shiraishi,[ab] G. Shoziyoev,[c] S. Simone,[r,s] M. Sioli,[w,t] C. Sirignano,[h,j]
G. Sirri,[t] M. Spinetti,[n] L. Stanco,[h] N. Starkov,[m] S.M. Stellacci,[i] M. Stipcevic,[ac] T. Strauss,[e]
P. Strolin,[b,q] K. Suzuki,[ab] S. Takahashi,[d] M. Tenti,[w] F. Terranova,[n,ak] V. Tioukov,[b]
P. Tolun,[z,†] S. Tufanli,[e] P. Vilain,[al] M. Vladimirov,[m] L. Votano,[n] J.-L. Vuilleumier,[e]
G. Wilquet,[al] B. Wonsak,[l] C.S. Yoon,[ae] J. Yoshida,[ab] Y. Zaitsev,[ai] S. Zemskova[o] and
A. Zghiche[k]

[a] INR-Institute for Nuclear Research of the Russian Academy of Sciences, RUS-117312 Moscow, Russia
[b] INFN Sezione di Napoli, I-80125 Napoli, Italy
[c] (MSU SINP) Lomonosov Moscow State University Skobeltsyn Institute of Nuclear Physics, RUS-119992 Moscow, Russia
[d] Kobe University, J-657-8501 Kobe, Japan
[e] Albert Einstein Center for Fundamental Physics, Laboratory for High Energy Physics (LHEP), University of Bern, CH-3012 Bern, Switzerland
[f] IPNL, Université Claude Bernard Lyon I, CNRS/IN2P3, F-69622 Villeurbanne, France
[g] ETH Zurich, Institute for Particle Physics, CH-8093 Zurich, Switzerland
[h] INFN Sezione di Padova, I-35131 Padova, Italy
[i] Dipartimento di Fisica dell'Università di Salerno and INFN "Gruppo Collegato di Salerno", I-84084 Fisciano Salerno, Italy
[j] Dipartimento di Fisica dell'Università di Padova, 35131 I-Padova, Italy
[k] LAPP, Université de Savoie, CNRS/IN2P3, F-74941 Annecy-le-Vieux, France
[l] Hamburg University, D-22761 Hamburg, Germany
[m] LPI-Lebedev Physical Institute of the Russian Academy of Science, RUS-119991 Moscow, Russia
[n] INFN - Laboratori Nazionali di Frascati, I-00044 Frascati (Roma), Italy
[o] JINR-Joint Institute for Nuclear Research, RUS-141980 Dubna, Russia

^{p} INFN - Laboratori Nazionali del Gran Sasso, I-67010 Assergi (L'Aquila), Italy

^{q} Dipartimento di Scienze Fisiche dell'Università Federico II di Napoli, I-80125 Napoli, Italy

^{r} INFN Sezione di Bari, I-70126 Bari, Italy

^{s} Dipartimento di Fisica dell'Università di Bari, I-70126 Bari, Italy

^{t} Dipartimento di Fisica dell'Università di Bologna, I-40127 Bologna, Italy

^{u} IPHC, Université de Strasbourg, CNRS/IN2P3, F-67037 Strasbourg, France

^{v} Toho University, J-274-8510 Funabashi, Japan

^{w} INFN Sezione di Bologna, I-40127 Bologna, Italy

^{x} Department of Physics, Technion, IL-32000 Haifa, Israel

^{y} Università degli Studi di Urbino "Carlo Bo", I-61029 Urbino - Italy

^{z} METU-Middle East Technical University, TR-06800 Ankara, Turkey

^{aa} INFN Sezione di Roma, I-00185 Roma, Italy

^{ab} Nagoya University, J-464-8602 Nagoya, Japan

^{ac} IRB-Rudjer Boskovic Institute, HR-10002 Zagreb, Croatia

^{ad} Ankara University, TR-06100 Ankara, Turkey

^{ae} Gyeongsang National University, ROK-900 Gazwa-dong, Jinju 660-701, Korea

^{af} Aichi University of Education, J-448-8542 Kariya (Aichi-Ken), Japan

^{ag} Dipartimento di Fisica dell'Università di Roma Sapienza, I-00185 Roma, Italy

^{ah} Dipartimento di Fisica dell'Università dell'Aquila and INFN "Gruppo Collegato de L'Aquila", I-6710 L'Aquila, Italy

^{ai} ITEP-Institute for Theoretical and Experimental Physics RUS-117259 Moscow, Russia

^{aj} Utsunomiya University, J-321-8505 Utsunomiya, Japan

^{ak} Dipartimento di Fisica dell' Università di Milano-Bicocca, I-20126 Milano, Italy

^{al} IIHE, Université Libre de Bruxelles, B-1050 Brussels, Belgium

* Corresponding authors.

† Deceased.

^{1} Now at Deutsches Elektronen Synchrotron (DESY), 22607 Hamburg, Germany.

^{2} Now at Albert Einstein Center for Fundamental Physics, Laboratory for High Energy Physics (LHEP), University of Bern, CH-3012 Bern, Switzerland.

^{3} Now at Institute of Radiation Physics, University Hospital and University of Lausanne, CH-1007 Lausanne, Switzerland.

^{4} Now at Kyungpook National University, 80 Daehakro, Bukgu, Daegu, Republic of Korea.

^{5} Now at Dipartimento di Fisica, Università degli Studi Roma Tre, Roma I-00146, Italy.

^{6} Now at IPHC, Université de Strasbourg, CNRS/IN2P3, F-67037 Strasbourg, France.

^{7} Now at Samsung Changwon Hospital, Sungkyunkwan University, 158 Palyongro, MasanHoiwongu, Changwon, Republic of Korea.